Measurement of the Generalized Polarizabilities of the Proton in Virtual Compton Scattering at Q^2=0.92 and 1.76 GeV^2 : II. Dispersion Relation Analysis

G. Laveissière,[1] L. Todor,[2] N. Degrande,[3] S. Jaminion,[1] C. Jutier,[1,2] R. Di Salvo,[1] L. Van Hoorebeke,[3] L.C. Alexa,[4] B.D. Anderson,[5] K.A. Aniol,[6] K. Arundell,[7] G. Audit,[8] L. Auerbach,[9] F.T. Baker,[10] M. Baylac,[8] J. Berthot,[1] P.Y. Bertin,[1] W. Bertozzi,[11] L. Bimbot,[12] W.U. Boeglin,[13] E.J. Brash,[4] V. Breton,[1] H. Breuer,[14] E. Burtin,[8] J.R. Calarco,[15] L.S. Cardman,[16] C. Cavata,[8] C.-C. Chang,[14] J.-P. Chen,[16] E. Chudakov,[16] E. Cisbani,[17] D.S. Dale,[18] C.W. de Jager,[16] R. De Leo,[19] A. Deur,[1,16] N. d'Hose,[8] G.E. Dodge,[2] J.J. Domingo,[16] L. Elouadrhiri,[16] M.B. Epstein,[6] L.A. Ewell,[14] J.M. Finn,[7] K.G. Fissum,[11] H. Fonvieille,[1] G. Fournier,[8] B. Frois,[8] S. Frullani,[17] C. Furget,[20] H. Gao,[11,21] J. Gao,[11] F. Garibaldi,[17] A. Gasparian,[22,18] S. Gilad,[11] R. Gilman,[23,16] A. Glamazdin,[24] C. Glashausser,[23] J. Gomez,[16] V. Gorbenko,[24] P. Grenier,[1] P.A.M. Guichon,[8] J.O. Hansen,[16] R. Holmes,[25] M. Holtrop,[15] C. Howell,[21] G.M. Huber,[4] C.E. Hyde-Wright,[2] S. Incerti,[9] M. Iodice,[17] J. Jardillier,[8] M.K. Jones,[7,16] W. Kahl,[25] S. Kato,[26] A.T. Katramatou,[5] J.J. Kelly,[14] S. Kerhoas,[8] A. Ketikyan,[27] M. Khayat,[5] K. Kino,[28] S. Kox,[20] L.H. Kramer,[13] K.S. Kumar,[29] G. Kumbartzki,[23] M. Kuss,[16] A. Leone,[30] J.J. LeRose,[16] M. Liang,[16] R.A. Lindgren,[31] N. Liyanage,[11,31] G.J. Lolos,[4] R.W. Lourie,[32] R. Madey,[5] K. Maeda,[28] S. Malov,[23] D.M. Manley,[5] C. Marchand,[8] D. Marchand,[8] D.J. Margaziotis,[6] P. Markowitz,[13] J. Marroncle,[8] J. Martino,[8] C.J. Martoff,[9] K. McCormick,[2,23] J. McIntyre,[23] S. Mehrabyan,[27] F. Merchez,[20] Z.E. Meziani,[9] R. Michaels,[16] G.W. Miller,[29] J.Y. Mougey,[20] S.K. Nanda,[16] D. Neyret,[8] E.A.J.M. Offermann,[16] Z. Papandreou,[4] B. Pasquini,[33] C.F. Perdrisat,[7] R. Perrino,[30] G.G. Petratos,[5] S. Platchkov,[8] R. Pomatsalyuk,[24] D.L. Prout,[5] V.A. Punjabi,[34] T. Pussieux,[8] G. Quéménér,[7,20] R.D. Ransome,[23] O. Ravel,[1] J.S. Real,[20] F. Renard,[8] Y. Roblin,[1,16] D. Rowntree,[11] G. Rutledge,[7] P.M. Rutt,[23] A. Saha,[16] T. Saito,[28] A.J. Sarty,[35] A. Serdarevic,[4,16] T. Smith,[15] G. Smirnov,[1] K. Soldi,[36] P. Sorokin,[24] P.A. Souder,[25] R. Suleiman,[5,11] J.A. Templon,[10] T. Terasawa,[28] R. Tieulent,[20] E. Tomasi-Gustaffson,[8] H. Tsubota,[28] H. Ueno,[26] P.E. Ulmer,[2] G.M. Urciuoli,[17] M. Vanderhaeghen,[37,7,16] R. Van De Vyver,[3] R.L.J. Van der Meer,[4,16] P. Vernin,[8] B. Vlahovic,[36] H. Voskanyan,[27] E. Voutier,[20] J.W. Watson,[5] L.B. Weinstein,[2] K. Wijesooriya,[7] R. Wilson,[38] B.B. Wojtsekhowski,[16] D.G. Zainea,[4] W-M. Zhang,[5] J. Zhao,[11] and Z.-L. Zhou[11]

(The Jefferson Lab Hall A Collaboration)

[1] *Université Blaise Pascal/IN2P3, F-63177 Aubière, France*
[2] *Old Dominion University, Norfolk, VA 23529*
[3] *University of Gent, B-9000 Gent, Belgium*
[4] *University of Regina, Regina, SK S4S OA2, Canada*
[5] *Kent State University, Kent OH 44242*
[6] *California State University, Los Angeles, CA 90032*
[7] *College of William and Mary, Williamsburg, VA 23187*
[8] *CEA Saclay, F-91191 Gif-sur-Yvette, France*
[9] *Temple University, Philadelphia, PA 19122*
[10] *University of Georgia, Athens, GA 30602*
[11] *Massachusetts Institute of Technology, Cambridge, MA 02139*
[12] *Institut de Physique Nucléaire, F-91406 Orsay, France*
[13] *Florida International University, Miami, FL 33199*
[14] *University of Maryland, College Park, MD 20742*
[15] *University of New Hampshire, Durham, NH 03824*
[16] *Thomas Jefferson National Accelerator Facility, Newport News, VA 23606*
[17] *INFN, Sezione Sanità and Istituto Superiore di Sanità, 00161 Rome, Italy*
[18] *University of Kentucky, Lexington, KY 40506*
[19] *INFN, Sezione di Bari and University of Bari, 70126 Bari, Italy*
[20] *Laboratoire de Physique Subatomique et de Cosmologie, F-38026 Grenoble, France*
[21] *Duke University, Durham, NC 27706*
[22] *Hampton University, Hampton, VA 23668*
[23] *Rutgers, The State University of New Jersey, Piscataway, NJ 08855*
[24] *Kharkov Institute of Physics and Technology, Kharkov 61108, Ukraine*
[25] *Syracuse University, Syracuse, NY 13244*
[26] *Yamagata University, Yamagata 990, Japan*
[27] *Yerevan Physics Institute, Yerevan 375036, Armenia*
[28] *Tohoku University, Sendai 980, Japan*
[29] *Princeton University, Princeton, NJ 08544*
[30] *INFN, Sezione di Lecce, 73100 Lecce, Italy*
[31] *University of Virginia, Charlottesville, VA 22901*
[32] *State University of New York at Stony Brook, Stony Brook, NY 11794*

[33]DFNT, University of Pavia and INFN, Sezione di Pavia; ECT*, Villazzano (Trento), Italy
[34]Norfolk State University, Norfolk, VA 23504
[35]Florida State University, Tallahassee, FL 32306
[36]North Carolina Central University, Durham, NC 27707
[37]Institut fuer Kernphysik, University of Mainz, D-55099 Mainz, Germany
[38]Harvard University, Cambridge, MA 02138

Virtual Compton Scattering is studied at the Thomas Jefferson National Accelerator Facility in the energy domain below pion threshold and in the $\Delta(1232)$ resonance region. The data analysis is based on the Dispersion Relation (DR) approach. The electric and magnetic Generalized Polarizabilities (GPs) of the proton and the structure functions $P_{LL} - P_{TT}/\epsilon$ and P_{LT} are determined at four-momentum transfer squared Q^2= 0.92 and 1.76 GeV^2. The DR analysis is consistent with the low-energy expansion analysis. The world data set indicates that neither the electric nor magnetic GP follows a simple dipole form.

PACS numbers: 23.23.+x,56.65.Dy

Virtual Compton Scattering (VCS) $\gamma^* p \to \gamma p$ has developed in the last decade as a powerful tool to study the nucleon structure. At low CM-frame energy W, the VCS amplitude is parametrized as a function of the Generalized Polarizabilities (GPs) of the proton [1], which depend on the four-momentum transfer squared Q^2 of the virtual photon. These new observables have become the subject of experimental investigation via the study of photon electroproduction $ep \to ep\gamma$. In a companion Letter (referred to as I) we present an extraction of the structure functions $P_{LL} - P_{TT}/\epsilon$ and P_{LT} from data below $N\pi$ threshold [2], following the low-energy expansion (LEX) formalism [1].

B. Pasquini *et al.* recently developed a formalism for VCS based on Dispersion Relations (DRs) [3]. In this Letter we report a determination of the electric and magnetic GPs of the proton ($\alpha_E(Q^2)$ and $\beta_M(Q^2)$, respectively) from an analysis based on the DR model. The structure functions $P_{LL} - P_{TT}/\epsilon$ and P_{LT} are also extracted. The method uses the photon electroproduction cross section measured in the E93-050 experiment [4] at Jefferson Lab (JLab).

In the DR formalism, the VCS amplitude is predicted from the MAID parametrization [5] of pion electroproduction, π^0 and σ-meson t-channel exchange, plus two other Q^2-dependent functions (subtraction constants). The latter are unconstrained phenomenological contributions to $\alpha_E(Q^2)$ and $\beta_M(Q^2)$; therefore these GPs are not fixed by the DR model. They are written as:

$$\alpha_E(Q^2) \;=\; \alpha_E^{\pi N}(Q^2) \;+\; \frac{[\;\alpha_E^{exp} - \alpha_E^{\pi N}\;]_{Q^2=0}}{(\;1 + Q^2/\Lambda_\alpha^2\;)^2} \qquad (1)$$

(same relation for β_M with parameter Λ_β) where $\alpha_E^{\pi N}$ ($\beta_M^{\pi N}$) is the πN dispersive contribution evaluated using the MAID analysis, and α_E^{exp} (β_M^{exp}) is the experimental value at $Q^2 = 0$. The mass coefficients Λ_α and Λ_β are free parameters to be fitted experimentally. We note that the choice of a dipole form in Eq. 1 is not compulsory. A more fundamental property of the DR model is that, up to the $N\pi\pi$ threshold, it provides a rigorous treatment of the higher order terms in the VCS amplitude, beyond the lowest order GPs given by the LEX [1]. This feature allows the inclusion of data in the $\Delta(1232)$ resonance region in an extraction of GPs based on the DR approach.

The JLab experiment uses the 4 GeV Continuous Electron Beam Accelerator and the Hall A instrumentation [6]. More details can be found elsewhere [7, 8, 9, 10, 11, 12]. The present study involves all the ($ep \to ep\gamma$) events with $W < 1.28$ GeV. The events are divided into three independent subsets listed in Table I. For data sets I-a and II, by far most of the events lie below pion threshold; actually these two sets have also been used in the LEX analysis [2] considering only events such that $W < (M_p + M_\pi)$. Data set I-b covers mainly the $\Delta(1232)$ resonance region in W. The three data sets of Table I are the subject of three distinct DR analyses. The basic ingredients for the cross-section determination are common to all our analyses of this experiment [7, 8, 9, 10, 11, 12]. They include a dedicated Monte-Carlo simulation [13] to obtain the acceptance, proper cuts to eliminate background, the application of radiative corrections [14], the calibration of experimental offsets and the absolute normalization of the experiment. It is important to have a realistic shape for the sampling cross section in the Monte-Carlo in order to calculate an accurate solid angle. For this purpose, simulated events are sampled in the DR model cross section ($d^5\sigma^{DR}$) which reproduces the enhancement of the Δ resonance. $d^5\sigma^{DR}$ depends on two free parameters Λ_α and Λ_β (cf. Eq. 1) which are iteratively fitted by a χ^2 minimization at the cross section level. When W increases, the acceptance is reduced to backward polar angles $\theta_{\gamma^*\gamma CM}$ (angle between the virtual and the final photons in the (γp) CM frame). Cross-section data obtained in this angular region are shown in Figs. 1 and 2. Kinematical conditions are defined on

TABLE I: Data sets for the DR analyses.

data set	Q^2-range (GeV^2)	W-range
I-a	[0.85, 1.15]	mostly $< \pi N$ threshold
I-b	[0.85, 1.15]	mostly Δ resonance
II	[1.60, 2.10]	mostly $< \pi N$ threshold

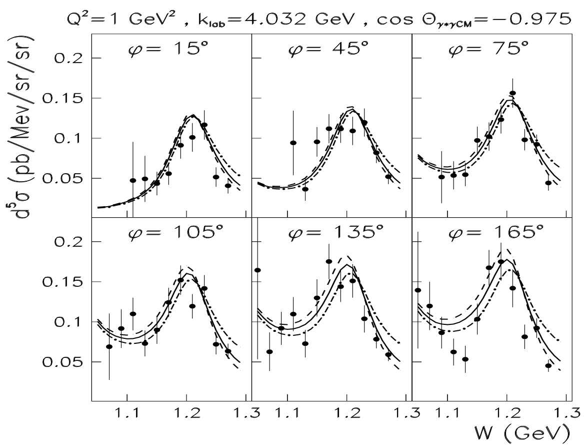

FIG. 1: $(ep \to ep\gamma)$ cross section for data set I-b in six intervals of the azimuthal angle φ (angle between lepton and hadron planes) as a function of W. By symmetry the statistics for φ= 180° to 360° are also included. Only statistical errors are shown. The solid curve is the prediction of the DR model for parameter values (Λ_α, Λ_β)=(0.7, 0.6) GeV, while the dashed curve is for (0.5, 0.4) GeV and the dash-dotted curve for (0.9, 0.8) GeV, respectively.

the plots, k_{lab} being the incoming beam energy (Fig. 1), q the virtual photon CM momentum and ϵ the virtual photon polarization (Fig. 2). Figure 1 clearly shows the Δ resonance excitation and the various curves indicate the sensitivity of the DR model to its free parameters. In contrast with Fig. 1, Fig. 2 shows how the Bethe-Heitler+Born calculation, or the addition of a first-order GP effect as in the LEX approach [2], fails to reproduce the measured cross section above pion threshold.

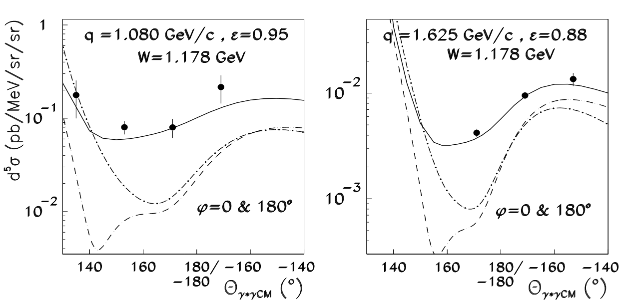

FIG. 2: $(ep \to ep\gamma)$ cross section for data sets I-a (left) and II (right). The outgoing photon is emitted in the lepton plane ($\varphi = 0°$ or 180°). The abscissa is the polar angle $\theta_{\gamma^*\gamma CM}$, with negative values corresponding to $\varphi = 180°$ as in Ref. [15]. Only statistical errors are shown. The full curve is the DR model prediction using the values of (Λ_α, Λ_β) fitted to each of the two data sets (see Table II). The dashed (dash-dotted) curve is the BH+Born (plus a first-order GP effect) cross section.

The results for Λ_α and Λ_β are presented in Table II. Systematic errors are calculated from the same four uncertainties as in the LEX analysis [2]. The resulting error bars differ from one data set to another; this comes from the various data sets having a different phase space coverage, and a different sensitivity to both the physics and the sources of systematic errors. The reasonably good χ^2 of the fits (1.3 to 1.5) indicates that the DR model works well in our kinematics and allows a reliable extraction of GPs, both below and above pion threshold. The compatibility between the three fitted values of Λ_α within errors (same for Λ_β) suggests that the dipole form of Eq. 1 is rather realistic, at least in the range $Q^2 \sim$ 1-2 GeV^2. We also note the close agreement between the obtained values of Λ_α and Λ_β.

In the DR model these results directly translate into values for the electric and magnetic GPs, using Eq. 1. Table II gives the result of this evaluation of $\alpha_E(Q^2)$ and $\beta_M(Q^2)$ at Q^2= 0.92 GeV^2 (data sets I-a and I-b) and Q^2= 1.76 GeV^2 (data set II). These points are shown in Fig. 3 together with the point at Q^2= 0 [16] and the points derived from the LEX analyses [2, 15]. It must be noted that the latter do not directly yield the GPs, but the structure functions $P_{LL} - P_{TT}/\epsilon$ and P_{LT}, which are combinations of GPs. Therefore to obtain the "LEX points" of Fig. 3 we have extracted $\alpha_E(Q^2)$ and $\beta_M(Q^2)$ from the measured structure functions [2, 15] according to the formulas [3]:

$$P_{LL} - \frac{1}{\epsilon} P_{TT} = \frac{4M_p}{\alpha_{\rm QED}} G_E^p\ \alpha_E(Q^2) + \text{ [spin-flip GPs]} \quad (2)$$

$$P_{LT} = -\frac{2M_p}{\alpha_{\rm QED}} \sqrt{\frac{q^2}{Q^2}} G_E^p\ \beta_M(Q^2) + \text{ [spin-flip GPs]} \quad (3)$$

where $\alpha_{\rm QED}$ is the fine-structure constant and G_E^p is the proton electric form factor. In this extraction the spin-flip GP terms are predicted by the DR model (so the result is model-dependent) and the parametrization of G_E^p is taken from Ref. [17]. The solid curve on Fig. 3 is the full DR calculation, split into its dispersive πN contribution (dashed curve) and the remaining asymptotic contribution (dash-dotted curve, dipole term of Eq. 1) for

TABLE II: Upper part: dipole mass parameters Λ_α and Λ_β obtained by fitting the three data sets independently. Lower part: electric and magnetic GPs evaluated at Q^2= 0.92 GeV^2 (data sets I-a, I-b) and 1.76 GeV^2 (data set II). The first and second errors are statistical and total systematic errors, respectively.

data set	Λ_α (GeV)	Λ_β (GeV)
I-a	0.741 ± 0.040 ± 0.175	0.788 ± 0.041 ± 0.114
I-b	0.702 ± 0.035 ± 0.037	0.632 ± 0.036 ± 0.023
II	0.774 ± 0.050 ± 0.149	0.698 ± 0.042 ± 0.077
data set	$\alpha_E(Q^2)$ (10^{-4}fm^3)	$\beta_M(Q^2)$ (10^{-4}fm^3)
I-a	1.02 ± 0.18 ± 0.77	0.13 ± 0.15 ± 0.42
I-b	0.85 ± 0.15 ± 0.16	0.66 ± 0.11 ± 0.07
II	0.52 ± 0.12 ± 0.35	0.10 ± 0.07 ± 0.12

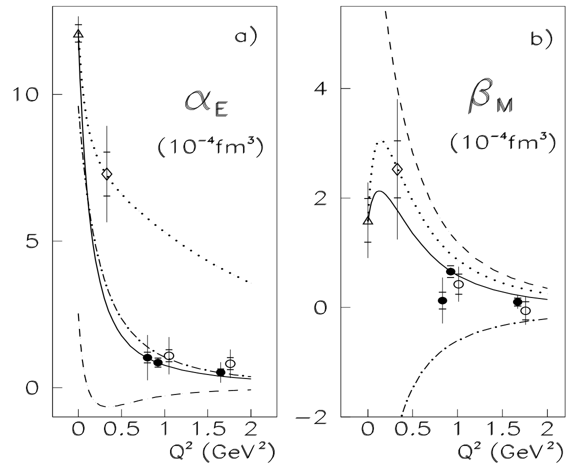

FIG. 3: Compilation of the data on electric (a) and magnetic (b) GPs. Data points are from Refs. [16] (△), the LEX analyses of MAMI [15] (◇) and JLab [2] (○) and the present DR results (•). Some JLab points are shifted in abscissa for better visibility. The inner error bar is statistical; the outer one is the total error (quadratic sum of statistical and systematic errors). The curves show the results of calculations in the DR model (see text).

Λ_α=0.70 GeV and Λ_β=0.63 GeV, as fitted on the JLab data set I-b. The πN intermediate states contribute very little to the electric polarizability at finite Q^2 (Fig. 3-a) and they create a small dia-electric effect ($\alpha_E^{\pi N} < 0$). The πN contribution to the magnetic polarizability in Fig. 3-b is strongly paramagnetic, predominantly arising from the $\Delta(1232)$ resonance. In the DR formalism, this is cancelled by a strong diamagnetic term originating from σ-meson t-channel exchange, and parametrized by Λ_β. The dotted curve is the full DR calculation evaluated for Λ_α=1.79 GeV and Λ_β=0.51 GeV, which reproduces the MAMI LEX data. The fact that there is no unique value of (Λ_α, Λ_β) agreeing with all data points suggests that the dipole form of Eq. 1, although working well in the range 1-2 GeV^2 as mentioned above, is not valid over the entire range of Q^2. This further suggests that the global behavior of the GP $\alpha_E(Q^2)$ does not follow a simple dipole form.

Finally, the results of our DR analyses can be expressed in terms of VCS structure functions. Using the GP values of Table II and the DR model prediction for P_{TT}, the structure functions $P_{LL} - P_{TT}/\epsilon$ and P_{LT} are determined from Eqs. 2 and 3. Their values are reported in Table III. To facilitate the comparison with the LEX results, the present determination is made at similar kinematics in Q^2 and ϵ (see Table III). The agreement with the values obtained in the LEX analysis [2] is very satisfactory. The results from the DR analysis of the (I-b) data set, obtained in the Δ region, yields smaller error bars due to an enhanced sensitivity to the GPs.

In summary we have analyzed the process $ep \to ep\gamma$ at JLab using a Dispersion Relation approach. The VCS structure functions obtained in this approach are in good agreement with the ones extracted using the low-energy expansion. We performed the first determination of GPs by analyzing data in the $\Delta(1232)$ resonance region. This opens up new possibilities to extract GPs from experiments, especially at higher Q^2.

We thank the JLab accelerator staff and the Hall A technical staff for their dedication. This work was supported by DOE contract DE-AC05-84ER40150 under which the Southeastern Universities Research Association (SURA) operates the Thomas Jefferson National Accelerator Facility. We acknowledge additional grants from the US DOE and NSF, the French Centre National de la Recherche Scientifique and Commissariat à l'Energie Atomique, the Conseil Régional d'Auvergne, the FWO-Flanders (Belgium) and the BOF-Gent University. We thank for the hospitality of ECT* (Trento) during VCS workshops where this work was discussed.

TABLE III: VCS structure functions obtained by the DR analyses of the three data sets. The first and second errors are statistical and total systematic errors, respectively.

data set	Q^2 (GeV^2)	ϵ	$P_{LL} - P_{TT}/\epsilon$ (GeV^{-2})	P_{LT} (GeV^{-2})
I-a	0.92	0.95	**1.70**	**-0.36**
			± 0.21 ± 0.89	± 0.10 ± 0.27
I-b	0.92	0.95	**1.50**	**-0.71**
			± 0.18 ± 0.19	± 0.07 ± 0.05
II	1.76	0.88	**0.40**	**-0.087**
			± 0.05 ± 0.16	± 0.019 ± 0.034

[1] P. A. M. Guichon, G. Q. Liu, and A. W. Thomas, Nucl. Phys. **A591**, 606 (1995).
[2] S. Jaminion et al., Letter I, to be submitted to Phys. Rev. Lett.
[3] B. Pasquini, M. Gorchtein, D. Drechsel, A. Metz, and M. Vanderhaeghen, Eur. Phys. J. **A11**, 185 (2001).
[4] P. Y. Bertin, C. Hyde-Wright, P. A. M. Guichon, et al. (1993), experiment E93-050, URL `http://hallaweb.jlab.org/experiment/E93-050/vcs.html`.
[5] D. Drechsel, O. Hanstein, S. S. Kamalov, and L. Tiator, Nucl. Phys. **A645**, 145 (1999), URL `http://www.kph.uni-mainz.de/MAID/`.
[6] J. Alcorn et al., accepted by NIM A.
[7] G. Laveissière et al. (2003), to be submitted to Phys. Rev. C, nucl-ex/0308009.
[8] N. Degrande, Ph.D. thesis, Gent University (2001).
[9] S. Jaminion, Ph.D. thesis, Université Blaise Pascal (2001), DU 1259.

[10] C. Jutier, Ph.D. thesis, Old Dominion University and Université Blaise Pascal (2001), DU 1298.
[11] G. Laveissière, Ph.D. thesis, Université Blaise Pascal (2001), DU 1309.
[12] L. Todor, Ph.D. thesis, Old Dominion University (2000).
[13] L. Van Hoorebeke et al., to be submitted to NIM A.
[14] M. Vanderhaeghen, J. M. Friedrich, D. Lhuillier, D. Marchand, L. Van Hoorebeke, and J. Van de Wiele, Phys. Rev. **C62**, 025501 (2000).
[15] J. Roche et al., Phys. Rev. Lett. **85**, 708 (2000).
[16] V. Olmos de Leon et al., Eur. Phys. J. **A10**, 207 (2001).
[17] E. J. Brash, A. Kozlov, S. Li, and G. M. Huber, Phys. Rev. **C65**, 051001 (2002).